BIOGENESIS AND STRUCTURE OF GOLGI-DERIVED CELLULOSIC SCALES IN *PLEUROCHRYSIS.* II. SCALE COMPOSITION AND SUPRAMOLECULAR STRUCTURE*

DWIGHT K. ROMANOVICZ and R. MALCOLM BROWN, JR.

Department of Botany,
University of North Carolina,
Chapel Hill, N.C. 27514

SYNOPSIS

Intact *Pleurochrysis* scales can be obtained in cell-free preparations for physical and chemical characterization. Isolation of the scale subcomponents has been achieved by serial extraction with trifluoroacetic acid, correlated with negative staining to observe the extent of extraction. Compositional analysis of the radial and amorphous subcomponents has revealed the presence of glucose, galactose, arabinose, and fucose, as well as a peptide constituent amounting to approximately 10% by weight. The spiral microfibrils are cellulosic, as confirmed by infrared absorption and x-ray diffraction, and are coated with glycopeptide rich in hydroxyproline.

Observations of negatively stained preparations of isolated scales demonstrate that the intact cellulosic microfibril is a continuous ribbon 37 × 50 Å in cross-section and attaining a length of approximately 14 microns. With improved techniques yielding higher resolution (Bacitracin, uranyl acetate), the individual cellulose microfibril is resolved into four apparent protofibrils each 12 × 16 Å in cross-section. From these data, a macromolecular model of scale cellulose is proposed, incorporating assumptions about the protein moiety derived from positive staining characteristics, and crystallinity data calculated from wide angle x-ray diffraction and infrared absorption.

INTRODUCTION

The compact cell wall of *Pleurochrysis* is composed of Golgi-derived subunits called scales. Brown and co-workers [2] used negative staining of isolated scales to demonstrate the presence of three scale subcomponents: the radial microfibrils, the spiral microfibrils, and the amorphous polysaccharide coating. Continued investigation yielded an accumulation of data which suggested that the alkali-resistant spiral microfibrils were cellulosic in nature [3], but there was considerable lack of acceptance as a result of the general conviction that cellulose synthesis does

* Research presented in this paper was part of a Ph.D. dissertation submitted to the Department of Botany at the University of North Carolina in Chapel Hill, and was supported in part by an NDEA Title IV Fellowship (D.K.R.) and the National Science Foundation (GB 40937 to R.M.B.).

Applied Polymer Symposium No. 28, 587–610 (1976)

not occur via the Golgi apparatus [7]. Herth et al. [17] then undertook a careful study of the chemical composition of alkali-purified spiral microfibrils and confirmed the presence of a cellulosic structural polysaccharide, covalently linked with a peptide moiety. However, the absence of unequivocal crystallographic evidence still generates considerable doubt regarding the presence of cellulose (Preston, pers. comm.). In the present study, careful correlation between chemical extraction and negative staining has permitted a separation of the scale subcomponents for physical and chemical characterization, with special attention given to acid-purified scale cellulose.

EXPERIMENTAL

Axenic cultures of *Pleurochrysis scherffelii* Pringsheim were maintained on an agarized marine medium as described in the previous paper [5]. The cell-free scale preparation, scale fraction A [3], was obtained through zoospore release. When three-week-old vegetative cultures were flooded with artificial seawater (40 gms Rila/liter), the cells would divide and their products escape into the liquid as naked, free-swimming zoospores, leaving behind the thick vegetative cell wall. The liquid from such flooded cultures was briefly sonicated to disrupt the clumped scales, centrifuged at 1900 g to remove whole cells, and then centrifuged for 30 minutes at 40,000 g to pellet scale fraction A. After several washings with distilled water, this fraction was used for physical and chemical tests to determine the composition and structure of the scale subcomponents.

Analysis of Scale Structure and Composition

Negatively stained preparations were made with either 2% aqueous phosphotungstic acid (PTA) neutralized with 1N sodium hydroxide, or 2% aqueous uranyl acetate (UA). To improve the spreading of the stain, the wetting agent bacitracin (USP) was added to either the specimen or the staining solution at a final concentration of 300 μg/ml [14]. Specimen suspensions were mixed with the negative stain and mounted by the drop method on Formvar-carbon coated grids. For measurement of microfibrillar dimensions, selected areas were photographed on an Hitachi HU11E electron microscope at 75 kV and instrumental magnifications of 48,000 to 89,000. The negatives were printed on a Durst enlarger and dimensions were measured from the enlarged prints with a stereo microscope equipped with a filar eyepiece. All measurements were calibrated with the 84.4Å period of beef liver catalase (Ted Pella Co.) and the 110Å outer diameter of the ferritin molecule (Polysciences, Inc.), used both as internal and as external standards [15].

X-ray diffraction patterns were obtained photographically using a Searle toroid camera and Ni-filtered CuK_α radiation from an Elliott rotating target generator. Films thus exposed were analyzed with a Joyce-Loebel microdensitometer for determination of spacings, intensities, and line widths. In order that all reflections could be recorded, regardless of intensity, each exposure was made on two layers of film. Specimen-to-film distance and instrumental line broadening were calibrated with the 2.82Å reflection of sodium chloride.

Infrared spectra were obtained with a Perkin-Elmer 457 grating spectrophotometer. Specimens were pressed into thin films on a glass surface and then removed with a razor blade after drying at least 72 hours over calcium chloride. For comparison, cotton fibers (*Gossypium hirsuitum* deltapine 16) from unopened bolls, approximately 30 days postanthesis, were treated in the same manner as scale material.

The density of acid-purified scale cellulose (extracted with 2N trifluoroacetic acid) was determined by suspending samples in a solution of toluene and methyl iodide. With small additions of either solvent, the solution was brought to a density equivalent with that of the sample as judged by lack of movement of the sample through the solution. The density of the solution was then determined with a pycnometer. The samples of scale cellulose were preconditioned in the following way: dried in a vacuum from a water-wet state (water dried); dehydrated with ethanol, transferred to toluene, then dried in a vacuum (toluene dried); dehydrated with ethanol and transferred to toluene (never dried = never removed from solvent). All samples were then soaked in toluene for at least 24 hours before density determination.

In order to determine the composition of the scale subcomponents, a serial extraction protocol was devised, using increasing concentrations of trifluoroacetic acid (TFA). Each step was monitored with negative staining to determine the extent of extraction (the protocol will be presented in detail in the Results section). The extracts were analyzed with the phenol-sulfuric acid test for total sugars [11] and the ninhydrin test for free amino acids [39]. Individual monosaccharide constituents were separated with thin-layer chromatography (Baker Cellulose Sheets No. 4468) and visualized with a mixture of 1.23 gm p-anisidine and 1.66 gm phthalic acid in 100 ml ethanol. The developing solvent was 1-butanol/pyridine/water (6:4:3).

In addition to these analyses, two qualitative tests for acidic polysaccharides were employed. Untreated whole cells were stained with 0.5% Alcian blue at pH 2.5 and pH 0.5 [34], as were cells which had been methylated (1% hydrochloric acid in absolute methanol, 4 days room temperature) or methylated and saponified (0.1N potassium hydroxide, 30 minutes room temperature) prior to staining [10]. The results were observed with the light microscope. For electron microscopic visualization of acidic polysaccharides, cells were treated with a 1.2 mg/ml suspension of cationized ferritin (Miles, Yeda, Ltd.) [9], prior to fixation and embedment for ultrathin sectioning [5].

RESULTS

Chemical Analysis

Among the qualitative biochemical tests used by Brown et al. [3] were the cationic dyes Ruthenium red and Alcian blue, which were taken up by the wall of *Pleurochrysis,* indicating the presence of pectin-like acidic polysaccharide. With modification of the staining solution and cell pretreatment [10, 34], the Alcian blue stain yielded further information about the nature of the acidic polysaccharide. When the staining solution is used at pH 2.5, both carboxyl groups and sulfate groups are charged and can take up the stain. However, at a pH below 1.0,

TABLE I
Alcian Blue Staining[a]

Pretreatment	pH 2.5	pH 0.5
None	+	+
Acidic MeOH	–	–
Acidic MeOH-KOH	+	–

[a] + indicates staining, – indicates lack of staining.

the carboxyl groups are protonated and only sulfate groups will bind stain molecules. As the wall of whole *Pleurochrysis* cells stained positively at both pH values, the presence of sulfate groups was certain. Pretreatment with acidic methanol removes sulfate groups and methylates carboxyl groups, blocking staining at both pH values. In *Pleurochrysis* cells treated with acidic methanol, saponification with 0.1N potassium hydroxide restored staining at pH 2.5. The results, summarized in Table I, established the presence of both sulfate and carboxyl groups in the acidic polysaccharide(s) of the *Pleurochrysis* wall. Since this staining at the light microscope level would not permit any distinction between scale subcomponents, ultrastructural localization of acidic polysaccharide with cationized ferritin [9] was undertaken. As seen from Figures 2 and 3, the localization on extracellular scales was confined to the radial microfibrils.

Further characterization of the scale required separation of the individual scale subcomponents, which was easily monitored with negative staining. When scale

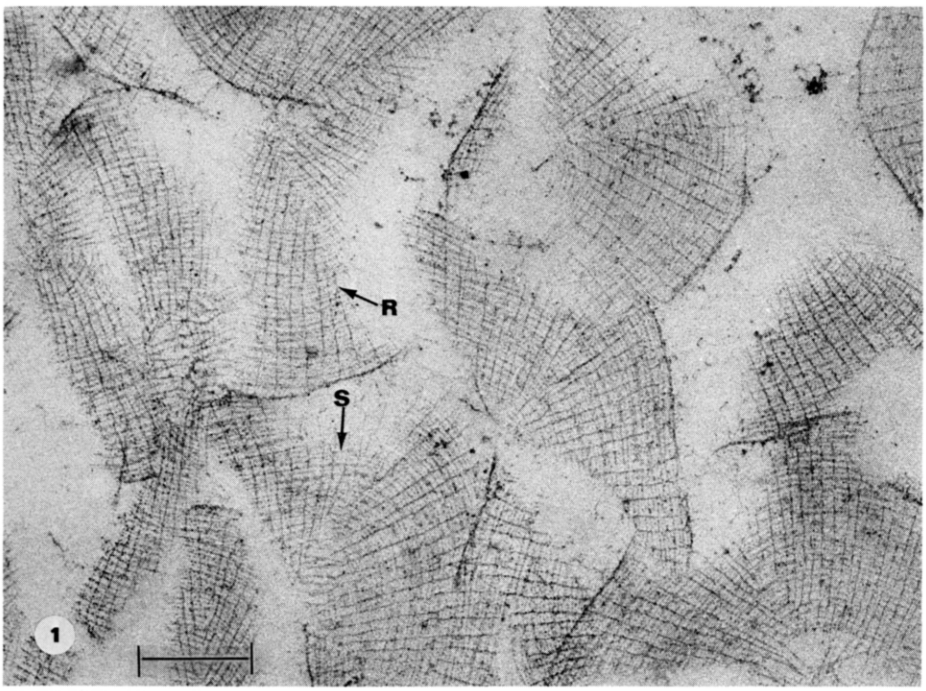

FIG. 1. Fixed scale material of *Pleurochrysis*, in section. Some scales are partially in the plane of the section, revealing both radial (R) and spiral (S) microfibrils. Standard fixation and embedment techniques. Magnification bar = 0.1 μm.

TABLE II
Chemical Analysis of Scale Subcomponents

Supernatant	Scale Subcomponent	Protein[a] %	Carbohydrate[b] %	Principal Monosaccharides[c]
1	amorphous polysaccharide	6	94	galactose, glucose, fucose
2	radial microfibrils	7	93	galactose, arabinose, fucose
3	spiral coating	9	91	galactose, glucose, mannose
4	spiral microfibrils	37	63	glucose

[a] Ninhydrin test for free amino acids.
[b] Phenol-sulfuric test for sugars.
[c] Thin-layer chromatography.

fraction A was observed directly, the amorphous polysaccharide often obscured the fibrillar subcompenents (Fig. 4). However, the treatment of the scale fraction A at 37°C with water made to pH 5.0 (with 0.1N TFA) hydrolyzed much of the amorphous subcomponent, permitting clear observation of the radial and spiral microfibrils (Fig. 5). Although this treatment would not remove all of the amor-

FIG. 2. Fixed scale material of *Pleurochrysis*, in section. Tangential section of scales treated with cationized ferritin, showing localization along the radial microfibrils. Magnification bar = 0.1 μm.

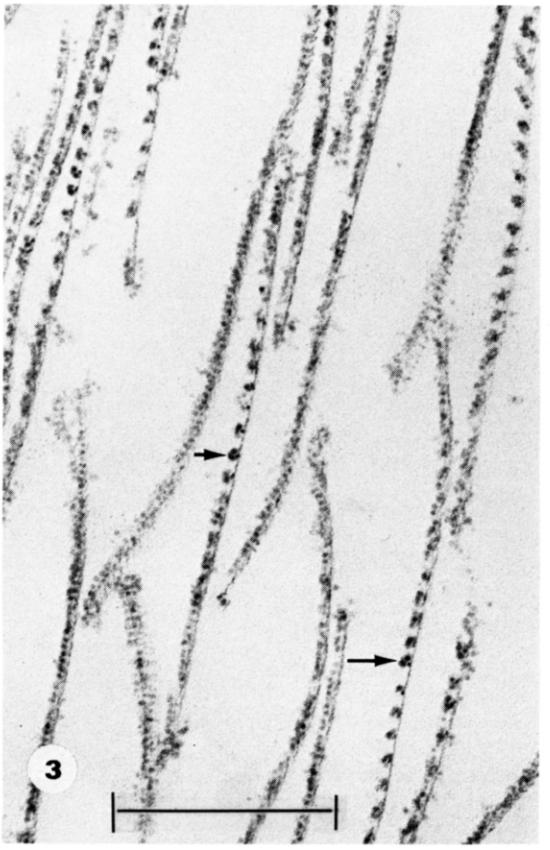

FIG. 3. Fixed scale material of *Pleurochrysis,* in section. Cross-section of scales treated with cationized ferritin, demonstrating localization around the radial microfibrils (arrows). Magnification bar = 0.1 μm.

phous subcomponent, it was chosen because any increase in acid concentration began to remove radial microfibrils. If the water-extracted scales were then treated with 0.5N TFA at 37°C, the radial microfibrils were hydrolyzed (see Figs. 9 and 10). Due to the apparent ease of solubility of the radial microfibrils, it was considered that this treatment might merely solubilize the bond between the radial microfibrils and the spiral microfibrils, removing the radial microfibrils from the scale without actually hydrolyzing them. However, the absence of any fibrillar structures in the 0.5 TFA supernatant (as judged by centrifugation at 60,000 g), and the presence of short pieces of radial microfibrils on some scales treated with 0.5N TFA (see Fig. 10), seemed to indicate that this treatment was indeed hydrolyzing the radial microfibrils. The next step in the sequential extraction was treatment with 2N TFA at 121°C (yielding acid-purified scale cellulose), which apparently removed a coating substance from the spiral microfibrils, as they no longer exhibited the spiral arrangement (see Fig. 12) and lost all positive stainability with electron stains. Uranyl acetate, lead citrate, osmium tetroxide, and osmium tetroxide—Ruthenium red all failed to produce an electron microscopic image of sectioned 2N TFA-extracted scales, whether used individually or in combination. Finally, the spiral microfibrils could be partially hydrolyzed by pro-

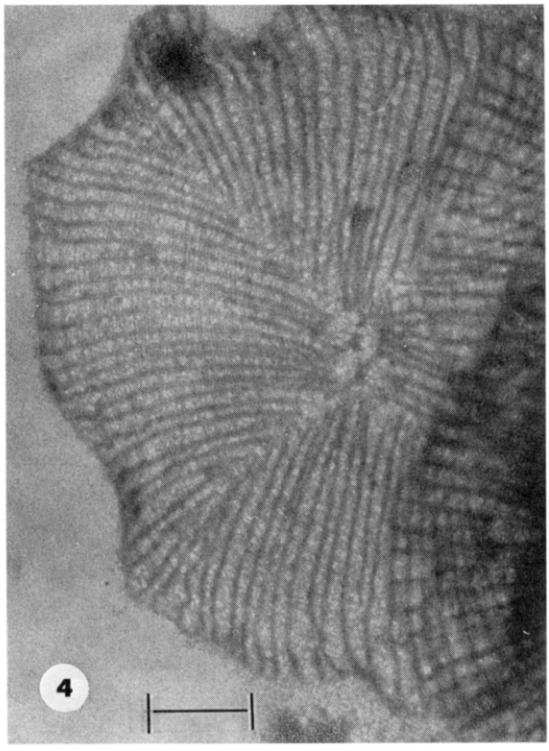

FIG. 4. Uranyl acetate negatively-stained preparations of isolated scales. Untreated scale fraction A. The radial pattern is evident, but radial microfibrils are masked by the presence of amorphous polysaccharide. Magnification bar = 0.1 μm.

longed treatment with 6N HCl at 100°C. A flow sheet of this serial extraction procedure is shown in Figure 16; between treatments the unhydrolyzed scale material was pelleted by 30 min centrifugation at 40,000 g.

As a result of the serial extraction, supernatants 1, 2, 3, and 4 contained hydrolysates of the amorphous subcomponent, the radial subcomponent, the spiral coating material, and the spiral subcomponent, respectively. Determination of the relative amounts (by weight) of carbohydrate and peptide by colorimetric analysis yielded the results presented in Table II. It was necessary to determine protein content as free amino acids from 6N HCl hydrolysis, because the paucity of aromatic amino acids causes a considerable underestimation of the protein content if the Folin method is used [17]. Thin-layer chromatography of the supernatants, and comparison with known standards, revealed the principal monosaccharide constituents of the subcomponents (Fig. 17). These results are also contained in Table II.

Physical Analysis

The dimensions of the radial and spiral microfibrils, normal to the microfibril axis, were measured from uranyl acetate negatively stained preparations. Since radial microfibrils were only observed while attached to the spiral network, only

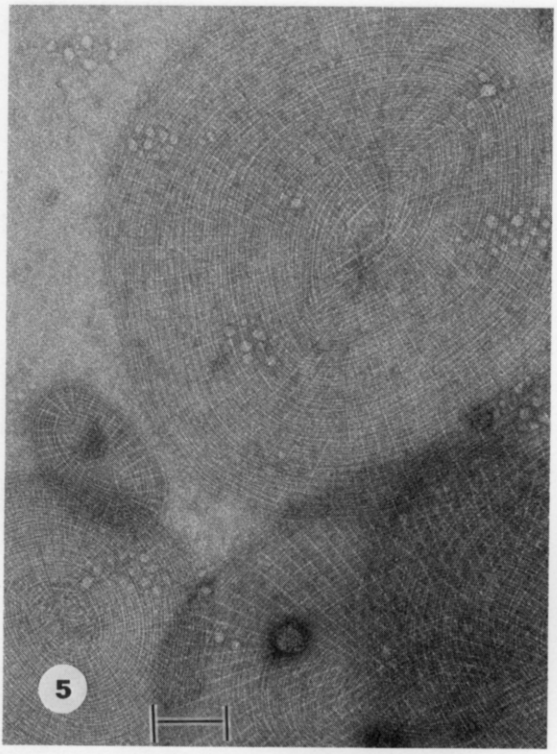

FIG. 5. Uranyl acetate negatively-stained preparations of isolated scales. Scale fraction A after treatment with water at pH 5. Both radial and spiral microfibrils are clearly visible. Note range of scale sizes. Magnification bar = 0.1 μm.

one dimension of the radial microfibril could be measured. When uranyl acetate was used as the negative stain, a dark central band was observed, extending the length of the radial microfibril (Figs. 7 and 8). Measurements were taken across the width of the radial microfibril and across the central band. A histogram of these measurements is presented in Figure 18; the mean and standard deviation of the microfibril width and central band width are presented in Table III.

Spiral microfibrils were measured from both native and 2N TFA-extracted scales, with uranyl acetate as the negative stain. The values for microfibril width

FIG. 6. Uranyl acetate negatively-stained preparations of isolated scales. A segment of an untreated scale, showing the dark central band of the spiral microfibrils (arrows). Magnification bar = 0.1 μm.

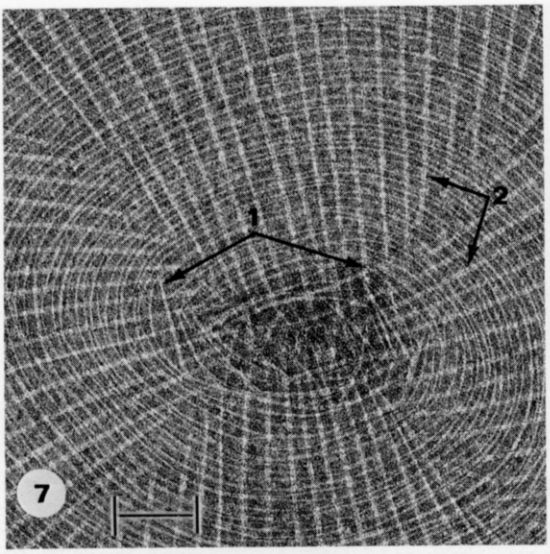

FIG. 7. Uranyl acetate negatively-stained preparations of isolated scales. A portion of a scale, showing breakage loci of the spiral microfibrils (1) and the dark central band of the radial microfibrils (2). Magnification bar = 0.1 μm.

fell into two size groups, indicating a rectangular cross-section as reported earlier by Brown et al. [3]. In the spiraling band arrangement of the native scale (Fig. 11), the spiral microfibril is oriented with the narrow axis parallel to the plane of the scale so that this axis is encountered more frequently than the broad axis which, in native material, can only be measured from twisted microfibrils. As demonstrated with the radial microfibrils, uranyl acetate revealed a dark central band on both surfaces of the spiral microfibrils (Figs. 6, 13, and 14). Measure-

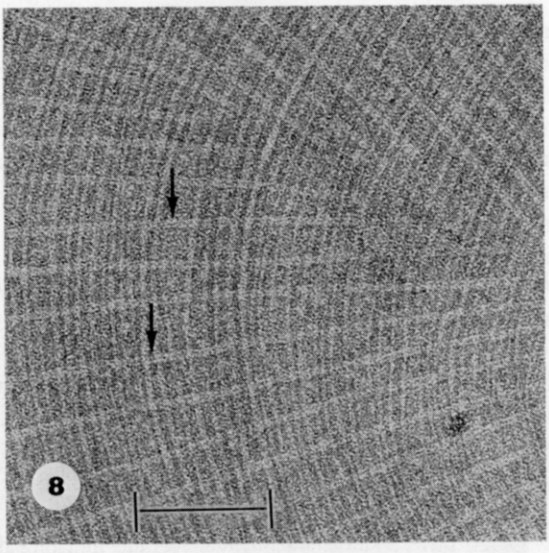

FIG. 8. Uranyl acetate negatively-stained preparations of isolated scales. A portion of a scale, revealing the dark central band of the radial microfibrils (arrows). Magnification bar = 0.1 μm.

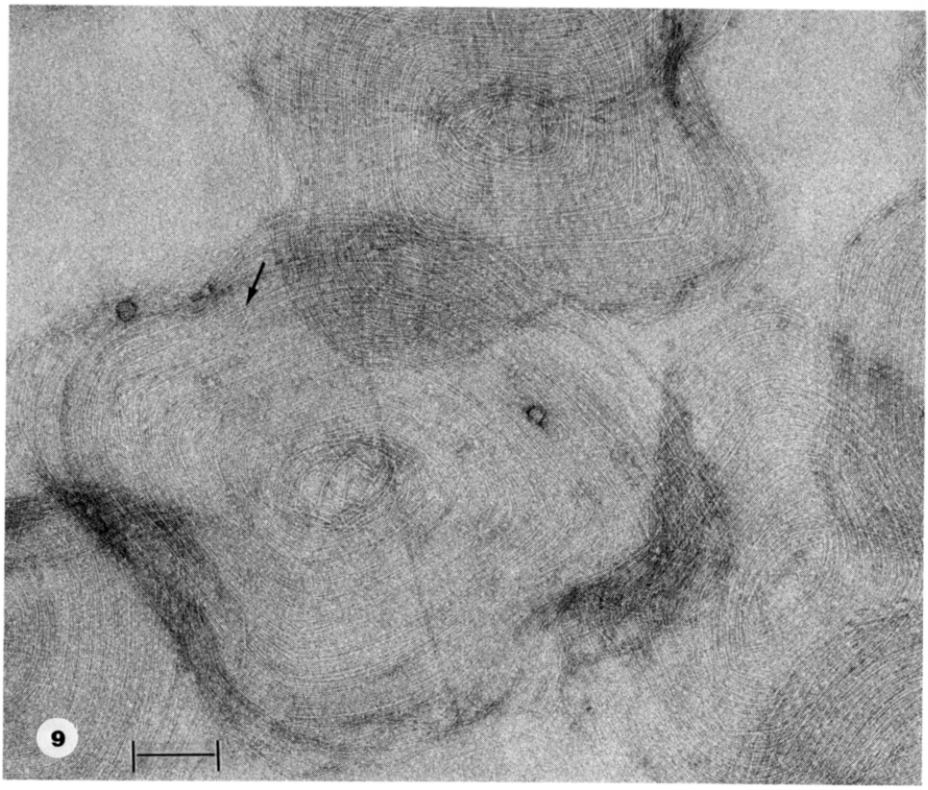

FIG. 9. Uranyl acetate negatively-stained preparation of scale fraction A after extraction with 0.5N trifluoroacetic acid. Radial microfibrils have been removed except for short fragments (arrows). Magnification bar = 0.1 μm.

ments were taken across the width of the spiral microfibril and across the central band (Fig. 19 and Table III). Statistical analysis (t-test) showed that the mean values were identical for native and 2N TFA-extracted spiral microfibrils, so the data from both were combined. In only one instance was there an indication of a split microfibril, revealing two of what could be four protofibrils in the spiral microfibril (Fig. 15 and Discussion).

In positively stained, ultrathin sections of native scales (Fig. 1), observed dimensions are somewhat larger than in negatively stained preparations: a mean width of 72Å (SD = 5Å) for the radial microfibrils and 62Å (SD = 3Å) for the spiral microfibrils. Since no twisting spiral microfibrils were observed, it is likely that positive staining of the spiral microfibril coating obscures the rectangular cross-section of crystalline core. As mentioned earlier, 2N TFA-extracted spiral microfibrils were not visible with positive staining in sectioned material. Thus, their dimensions with positive staining could not be determined.

X-ray diffraction patterns of native and 2N TFA-extracted scale material and cotton are shown in Figure 20, and the spacings measured from densitometer tracings in Table IV. Dried native scale fraction A yielded a single diffuse reflection containing two poorly defined maxima, and a weak 2.59Å reflection, indicative of β1-4 glucan. After the 2N TFA-extraction, wet scale material yielded a sharp

TABLE III
Microfibril Dimensions from Negative Staining

Microfibril	Total Width, Å	Central Band, Å
Radial	60 (4[a])	24 (4)
Spiral, native		
narrow[b]		
axis	37 (3)	11 (4)
broad[c]		
axis	49 (3)	17 (2)
Spiral, TFA-extracted[d]		
narrow		
axis	37 (2)	11 (1)
broad		
axis	49 (3)	16 (1)
Spiral, combined native and extracted		
narrow		
axis	37 (3)	11 (2)
broad		
axis	49 (3)	16 (1)

[a] Standard deviation, Å.
[b] Narrow axis, parallel to the plane of the scale.
[c] Broad axis, perpendicular to the plane of the scale.
[d] Extracted with 2N trifluoroacetic acid, 3 hours, 121°C.

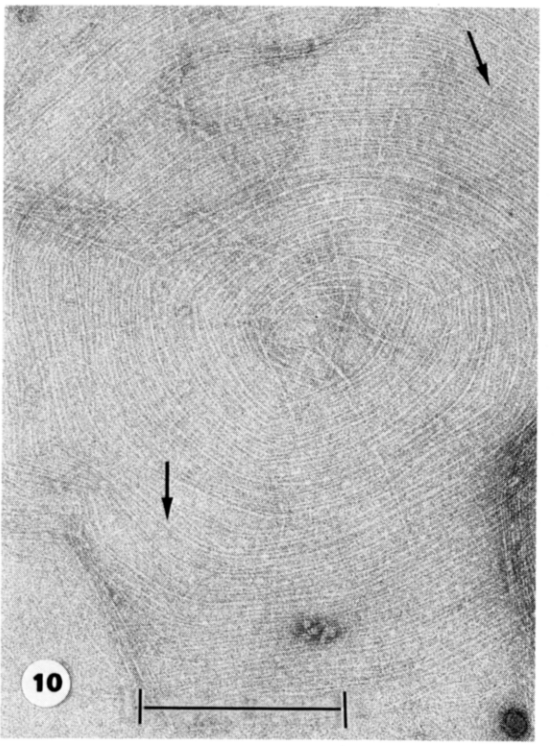

FIG. 10. Same as Figure 9.

TABLE IV
X-Ray Spacings, Å

Native Scales, Dried	Acid-Purified[a] Scales, Wet	Acid Purified[a] Scales, Dried	Cotton
		6.01M	6.07M
		5.40M	5.49M
4.91W		4.32W	4.35M
4.07W	3.92M	3.99S	3.97S
3.25VW		3.21VW	3.21VW
2.59VW		2.60W	2.60W

S = strong, M = medium, W = weak, VW = very weak.
[a] Extracted with 2N trifluoroacetic acid, 3 hours, 121°C.

3.9Å reflection inside the broad water band. Upon drying, the acid-purified scale material gave a complete cellulose I pattern.

Infrared spectra of native and 2N TFA-extracted scale material are shown in Figure 21, along with the spectra of native and 2N TFA-extracted cotton. While the overall similarity is obvious, several points deserve comment. In the 3000–3600 cm^{-1} region, assigned to OH stretching and indicative of hydrogen bonding [24, 27, 44], all four spectra reveal a broad absorption band which shifts slightly

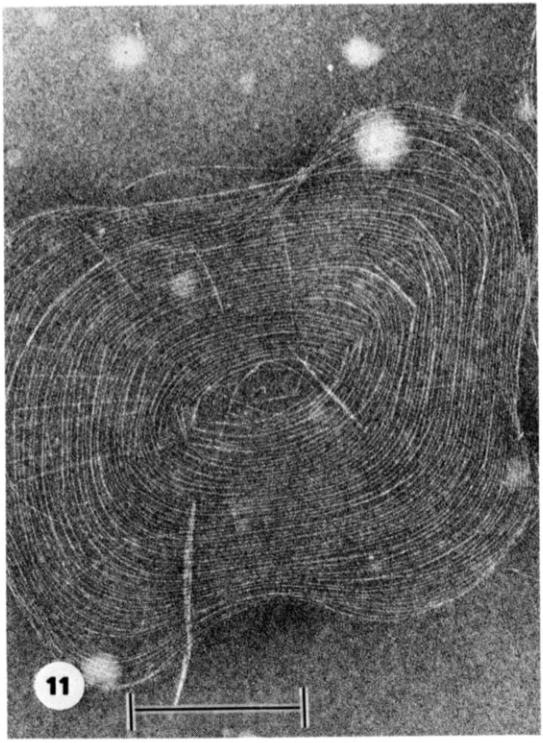

FIG. 11. Phosphotungstic acid negatively-stained preparation of scale fraction A after extraction with 1N hydrochloric acid. The spiraling band arrangement of the spiral microfibrils is evident. Magnification bar = 0.1 μm.

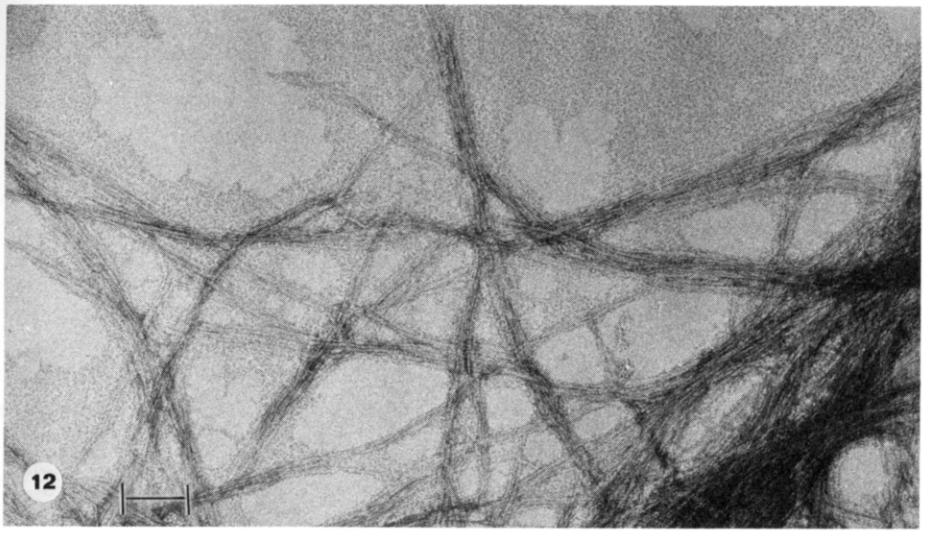

FIG. 12. Uranyl acetate negatively-stained preparations of scale fraction A after extraction with 2N trifluoroacetic acid. Survey of extracted scale material. Spiral microfibrils have lost the spiraling band arrangement, but do not appear to have been degraded in length. Magnification bar = 0.1 μm.

toward lower frequencies in the TFA-extracted material. The lack of distinct absorption frequencies is due to the low crystallinity of the samples (see Discussion), an interpretation supported by the observation that the more highly crystalline *Valonia* and bacterial cellulose yield as many as six bands in this region [24, 26, 27]. Zhbankov [46] has shown that absorption due to intramolecular hydrogen bonding occurs at higher frequencies than that due to intermolecular hydrogen bonding; thus, the shift toward lower frequencies in acid acid extracted material could also be indicative of an increase in crystallinity upon extraction.

The peaks in the 1600–1800 cm^{-1} region were assigned by Tsuboi [44] to adsorbed water in the material. Although O'Conner et al. [31] had suggested an assignment to C=O stretching, little further attention was paid to this region until a survey of infrared absorption by fungal walls showed it to be indicative of the presence of protein [28]. This interpretation is supported by chemical analysis of scale material presented above.

Lloyd et al. [25] have demonstrated that sulfated polysaccharides exhibit bands at 1240 and 820–850 cm^{-1}, assigned to S=O stretching and C–O–S vibrations,

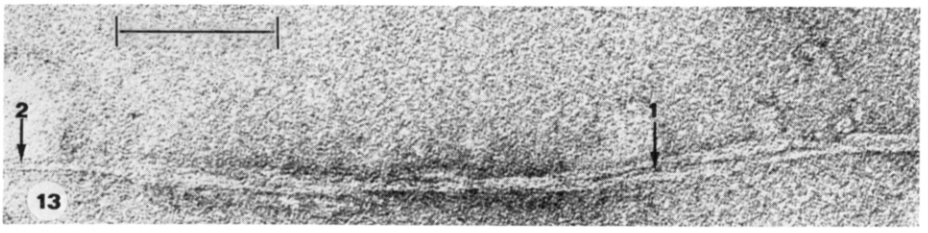

FIG. 13. Uranyl acetate negatively-stained preparations of scale fraction A after extraction with 2N trifluoroacetic acid. High resolution micrograph revealing the broad (1) and narrow (2) dimensions of the spiral microfibril, both with the dark central band. Magnification bar = 0.1 μm.

TABLE V
Density of Acid Purified[a] Scale Cellulose

Preconditioning	Density, gm/cc
Never-dried[b]	1.59
Toluene-dried[c]	1.57
Water-dried[d]	1.50

[a] Extracted with 2N trifluoroacetic acid, 3 hours, 121°C.
[b] Solvent exchanged to toluene.
[c] Solvent exchanged to toluene, dried.
[d] Dried from water (native solvent).

respectively. The absorption band near 1240 cm^{-1} has been recorded by other investigators but has not been unequivocally assigned. From the spectra in Figure 21, it can be seen that TFA-extraction results in a diminishing of the 1240 cm^{-1} band and a loss of additional absorption frequencies in the 850 cm^{-1} region, suggesting that these bands are attributable to sulfated, noncellulosic polysaccharides, the presence of which has already been established in *Pleurochrysis*

The density values in gm/cc for samples of acid-purified (2N TFA-extracted) scale cellulose are presented in Table V. Three determinations were made and the results averaged, the difference between separate determinations on similar sam-

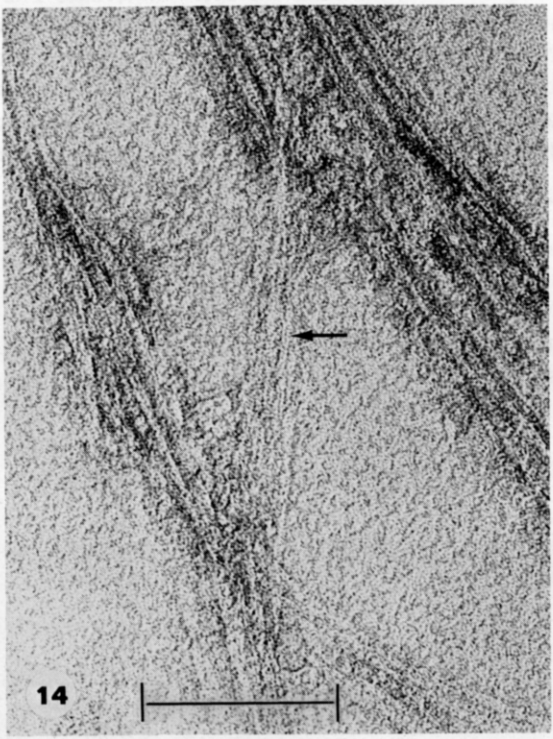

FIG. 14. Uranyl acetate negatively-stained preparations of scale fraction A after extraction with 2N trifluoroacetic acid. Two bundles of spiral microfibrils. The individual microfibril, with dark central band, can be observed in the central region (arrow) where there is no overlap of microfibrils. Magnification bar = 0.1 μm.

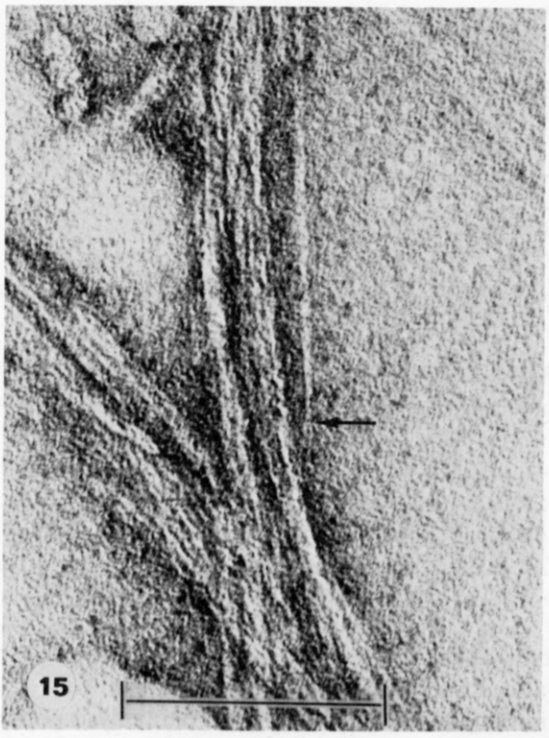

FIG. 15. Uranyl acetate negatively-stained preparations of scale fraction A after extraction with 2N trifluoroacetic acid. A single spiral microfibril which appears to split into two "protofibrils" (arrow). Magnification bar = 0.1 μm.

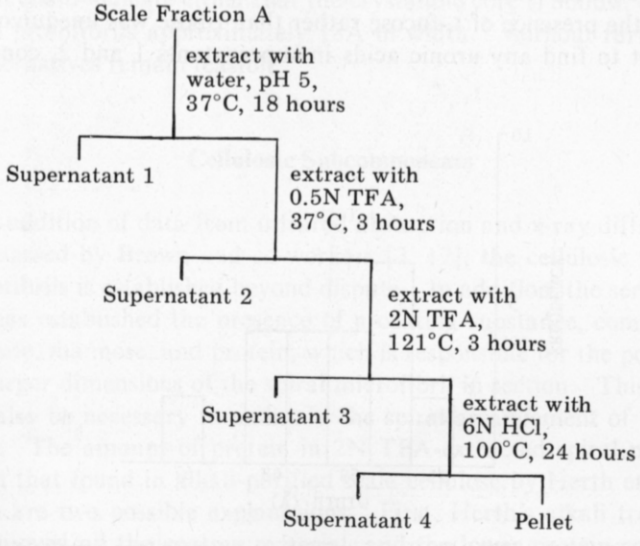

FIG. 16. Serial extraction protocol.

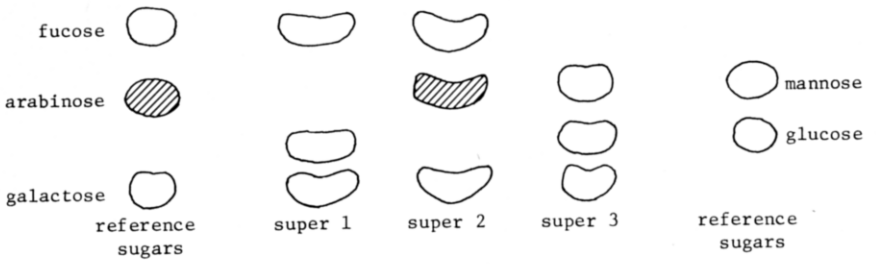

FIG. 17. Tracings from thin-layer chromatograms of scale fraction A extracts, pentose is shaded (////////).

ples being less than 0.01 gm/cc. For each day of determinations, the volume of the pycnometer was taken as the mean of three values obtained with distilled water.

DISCUSSION

Noncellulosic Subcomponents

The noncellulosic subcomponents—the amorphous polysaccharide and the radial microfibrils—are similar in solubility and staining properties (see silver methenamine staining in the previous paper). However, analysis of the monosaccharide constituents revealed that, while both contained galactose and L-fucose, the third constituent is glucose for the amorphous material and arabinose in the radial microfibrils. Brown et al. [3] demonstrated the presence of four monosaccharides in the noncellulosic scale material, which they identified as galactose, ribose, glucose, and arabinose. With the similarity in R_f values between ribose and L-fucose, it is understandable that the two would be confused, especially if the presence of L-fucose was not anticipated and a standard of it was not run. With the anisidine phthalate visualizer, ribose yielded a pink spot while L-fucose yielded a brown spot, so that the presence of L-fucose rather than ribose was unequivocal. It was surprising not to find any uronic acids in supernatants 1 and 2, considering the

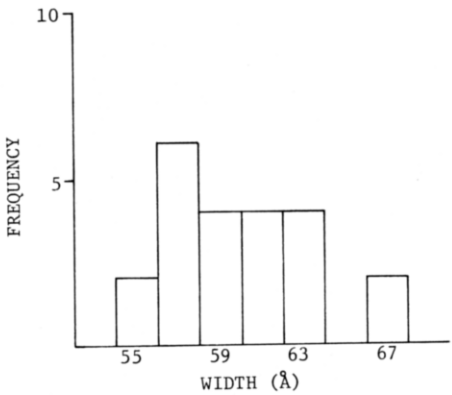

FIG. 18. Distribution of the width of radial microfibrils, as measured from negatively stained preparations.

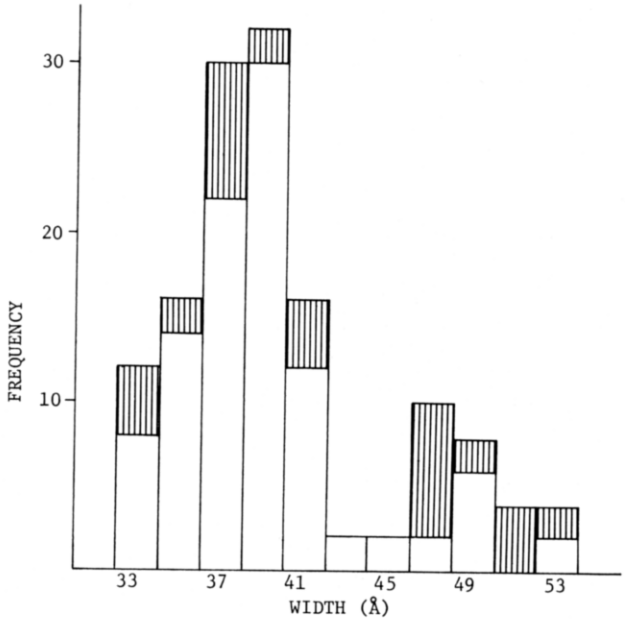

FIG. 19. Distribution of the width of spiral microfibrils, both native (clear) and 2N TFA-extracted (shaded), as measured from negatively stained preparations.

strong Alcian blue staining which remains after methylation and saponification. However, the presence of protein in the form of short polypeptides would account for the carboxyl groups indicated by the Alcian blue staining.

Concerning the structure of the radical microfibrils, the dark central band observed with uranyl acetate negative staining could be interpreted to represent a site of the protein moiety, binding the uranyl acetate and staining positively. If, on the other hand, there is no positive binding of uranyl acetate molecules, the dark central band could indicate either that the crystalline core is hollow, or that it consists of two protofibrils approximately 18Å in width. Without further evidence, all three alternatives remain feasible.

Cellulosic Subcomponents

With the addition of data from infrared absorption and x-ray diffraction to the evidence amassed by Brown and co-workers [3, 17], the cellulosic nature of the spiral microfibrils is established beyond dispute. In addition, the serial extraction procedure has established the presence of a coating substance, composed of glucose, galactose, mannose, and protein, which is responsible for the positive stainability and larger dimensions of the spiral microfibril in section. This coating material may also be necessary to maintain the spiral arrangement of the cellulosic microfibrils. The amount of protein in 2N TFA-extracted spiral microfibrils is greater than that found in alkali-purified scale cellulose by Herth et al. [17], for which there are two possible explanations. First, Herth's alkali treatment may not have removed all the coating material, and the lower protein content of this coating material would thus lower the overall protein percentage for the alkali-

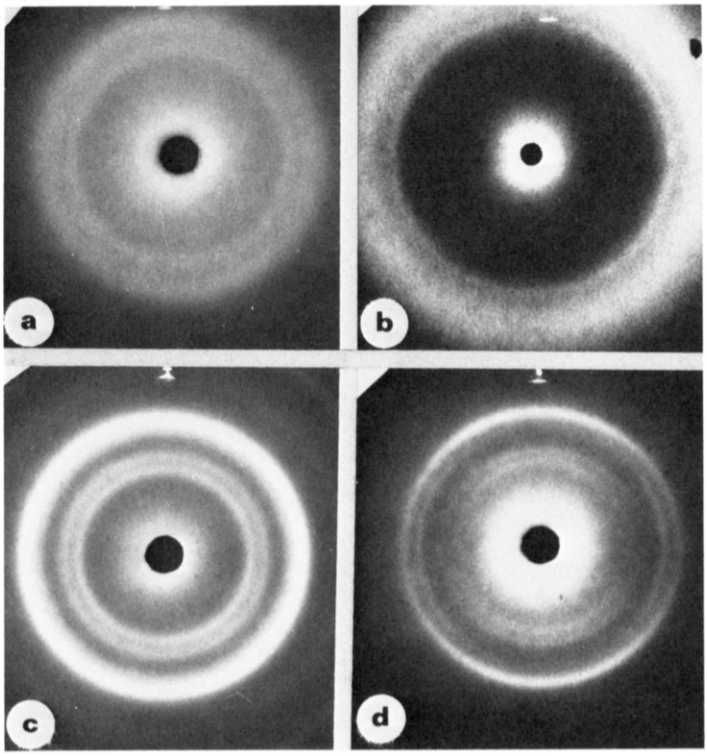

FIG. 20. X-ray diffraction patterns of scale and cotton cellulose: (a) Native scale fraction A, dried; (b) 2N TFA-extracted scale fraction A, wet; (c) 2N TFA-extracted scale fraction A, dried; (d) native cotton from dehiscent boll.

purified cellulose. On the other hand, the figure of 37% may be too high since the sugar content of supernatant 4 had to be determined after 6N HCl hydrolysis, a treatment which destroys an indeterminate amount of the sugar constituent, raising the apparent protein percentage. In either case, the presence of protein in scale cellulose is confirmed, a result which is important considering the increased interest in cell wall protein in recent years [4,8,18,37,40,43]. Lamport [22,23] has postulated a peptide called extensin based on the presence of hydroxyproline in cell walls from a number of sources [1,37,41]. In *Pleurochrysis* scales, the coating material of the cellulosic spiral microfibrils contains hydroxyproline as the most abundant amino acid residue (Lamport, pers. comm.). Since this coating material appears to be responsible for maintaining the spiral arrangement of the cellulosic microfibrils, it may be analogous to Lamport's extensin both in composition and function. It is also interesting to compare the composition of *Pleurochrysis* scales with the only other analysis of haptophycean scales, that of Green and Jennings [13] on the scales of *Chrysochromulina chiton.* Finding only galactose and ribose, and an x-ray diffraction pattern with a large number of indistinct reflections, they concluded that cellulose was not present. However, examination of their own micrographs of shadowed *Chrysochromulina* scales reveals that spiral microfibrils are present only in a narrow band at the rim of the scale. Thus, cellulose may be only a minor constituent of *Chrysochromulina* scales.

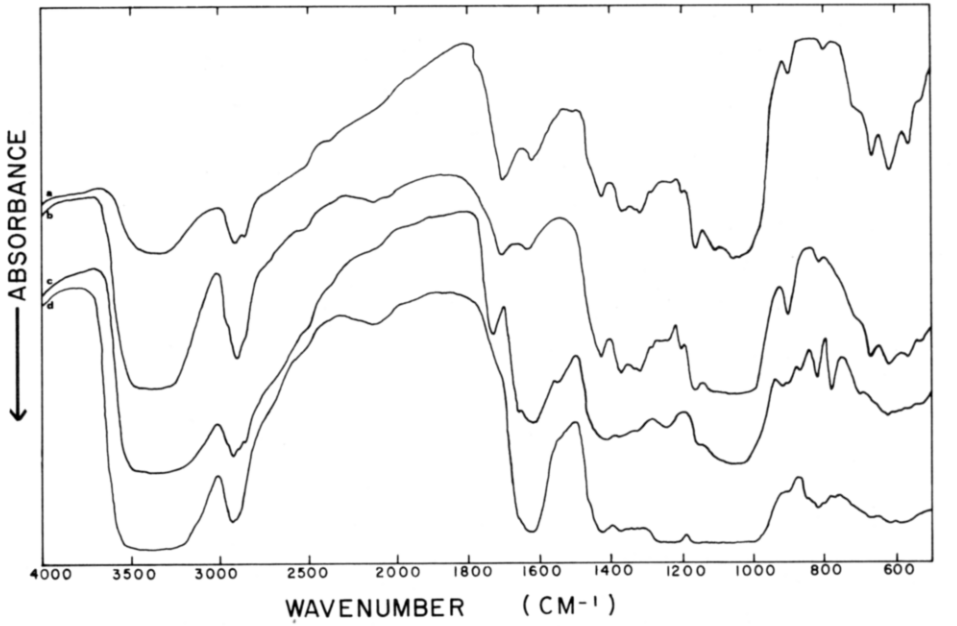

FIG. 21. Infrared absorption spectra of scale and cotton cellulose: (a) 2N TFA-extracted cotton; (b) 2N TFA-extracted scale cellulose; (c) native cotton; (d) native scale fraction A.

Acid-purified spiral microfibrils have dimensions identical to those of native spiral microfibrils, but the acid-purified spiral microfibrils are more crystalline, as indicated by x-ray diffraction and infrared absorption. Although absolute quantitation of crystallinity is not possible, estimates of relative crystallinity are useful in comparing different materials or the same material given different pretreatments. By comparison with other physical parameters which are sensitive to crystallinity, Segal et al. [42] devised an empirical method for calculating a crystallinity index from the intensity of reflections in x-ray diffraction patterns. This crystallinity index was defined as follows:

$$\text{Cr I} = \frac{(I_{002} - I_{am})}{I_{002}} \times 100$$

where I_{002} is the maximum intensity (in arbitrary units) of the 002 reflection ($2\theta = 24.4°$) and I_{am} is the intensity of diffraction in the same units at $2\theta = 18°$. Since $2\theta = 18°$ is the position of the maximum diffraction of amorphous cellulose, it is possible to have negative values. The crystallinity, as determined from infrared spectra, is calculated as the ratio between absorption at 1372 cm^{-1} and absorption at 2900 cm^{-1} [29]. In order that the two values may more easily be compared, the Segal values have been left as ratios rather than being converted to percentages as in the original equation. The calculated values are listed in Table VI, from which it is evident that acid extraction does indeed increase crystallinity. Since this increase in crystallinity is accompanied by a loss of positive stainability in section, but no alteration of the morphology of the crystalline core is observed with negative staining, it is possible that the acid extraction increases crystallinity simply by removing the noncrystalline coating material from the crystalline core. The values for cotton are rather low compared to those obtained in the studies

TABLE VI
Crystallinity of Scale and Cotton Cellulose

Sample	X-Ray[a]			Infrared[b]		
	I_{002}	I_{am}	Crystallinity	a_{1372}	a_{2900}	Crystallinity
Native scales	31	21	0.32	2	12	0.17
Acid-purified[c] scale cellulose	45	16	0.64	18	34	0.53
Native cotton	n.d.	n.d.	n.d.	2	37	0.05
Acid-purified[c] cotton cellulose	47	18	0.62	11	25	0.44

[a] Empirical formula: $Cr = (I_{002}-I_{am})/(I_{002})$, units arbitrary.

[b] $abs_{1372cm^{-1}}/abs_{2900cm^{-1}}$, units arbitrary.

[c] 2N trifluoroacetic acid, 3 hours, 121°C.

cited above. However, the cotton samples used in the present study were taken from unopened bolls, while those used by Segal et al. and Nelson and O'Conner had been processed commercially. From these data, it appears that there is greater similarity between scale cellulose and cotton cellulose with regard to crystallinity than between scale cellulose and the highly crystalline algal cellulose from *Valonia* [27].

The values obtained for the density of acid-purified scale cellulose vary considerably with the pretreatment. The highest value, that of solvent-exchanged never-dried material, is similar to the theoretical value of 1.592 calculated for cellulose by Hermans [16] from the unit cell dimensions. One explanation for the different values is related to the accessibility of scale cellulose to the solvent. Drying the scale material from its water-wet state causes a reduction in volume by a factor of about ten, and upon rewetting with toluene or water, there is virtually no regain of the lost volume. When dried from toluene after solvent exchange, some of the collapse is prevented, and upon rewetting with toluene the volume is restored to over half that of the never-dried, solvent-exchanged state. Thus, the greater the collapse, the less accessible the noncrystalline regions become to solvent penetration and the lower the density of the sample from that of crystalline cellulose. Orr et al. [33] observed a similar decrease in density with dried, solvent-exchanged cotton cellulose. They attributed the lower densities to a trapping of solvent molecules by the collapse of the cellulose structure. Both interpretations indicate a collapse upon drying which may be significant in correlating the data from negative staining and x-ray diffraction (see below).

Understanding the structure of the crystalline core of the spiral microfibril requires interpretation of the dark central band observed with uranyl acetate negative staining and correlation with other physical data. Since hydrolysis of acid-purified spiral microfibrils revealed the presence of a considerable amount of protein (37%), the microfibril may have a solid crystalline core with protein arranged on the surface that binds the UA. Alternately, the crystalline portion may consist of four 13 × 16Å protofibrils, stabilized by the peptide moiety into the 37 × 49Å spiral microfibril. Considering that the dark central band is not revealed by negative staining with PTA, but only by negative staining with the smaller uranyl acetate molecule (5Å) [15], the presence of the central band may be due to stain pen-

TABLE VII
Crystallite Size of Scale and Cotton Cellulose

Sample	Reflection	Observed Line Width,[b] deg	Corrected Line Width,[c] deg	Crystallite,[d] Å
Acid-purified[a] scales, dried	101 ($\theta = 7.4°$)	2.24	2.12	38
	$10\bar{1}$ ($\theta = 8.2°$)	2.26	2.14	38
	002 ($\theta = 11.2°$)	2.38	2.26	36
Cotton	101 ($\theta = 7.4°$)	1.95	1.80	45
	$10\bar{1}$ ($\theta = 8.2°$)	1.37	1.19	68
	002 ($\theta = 11.2°$)	1.68	1.51	54

[a] Extracted with 2N trifluoroacetic acid, 3 hours, 121°C.
[b] Peak width at one-half height.
[c] Corrected for instrumental line-broadening, b = 0.36°.
[d] Crystallite size = $(0.9\lambda)/(\beta\cos\theta)$, where β = line width, in radians.

etration rather than positive staining. This interpretation supports the protofibril model as well as a third model in which the protein is arranged on the surface of a solid crystalline core in such a configuration as to permit penetration by uranyl acetate. The three models are represented as diagrammatic cross-section in Figure 22.

An estimation of the lateral dimensions of the crystalline core (termed crystallite) can be obtained from the extent of line-broadening observed in x-ray diffraction patterns [21,37]. In theory, smaller crystallites result in broader lines; but in practice, line-broadening can also arise from the instrumental configuration and from disorder within the crystal. The calculated values in Table VII have been corrected for instrumental line-broadening [20], but since the disorder in cellulose cannot be quantified, these values represent a lower limit of the crystallite size. Although the absolute accuracy of this calculation is probably quite low [21], there is good agreement between the values obtained for cotton in this study (Table VII) and those obtained for cotton by other investigators [37]. Thus the values calculated for *Pleurochrysis* scale cellulose (Table VII) can be taken to indicate that scale cellulose has smaller crystallite dimensions than cellulose from any of the other plant sources studied to date [6, 30]. More importantly, these data support the overall dimensions of 37 × 49Å for the spiral microfibril, as obtained with negative staining.

In terms of the three alternatives presented in Figure 22, the line-broadening data support a microfibril with a solid crystallive core. However, these data were obtained from dried scale material which, according to the density determinations, may be considerably collapsed from the wet state. This collapse upon drying could result in larger crystallites as was demonstrated in cotton cellulose [35], but not in the algal cellulose from *Valonia* [6] or *Chaetomorpha* [30]. In contrast, the negative staining data were obtained from samples which were mixed with the

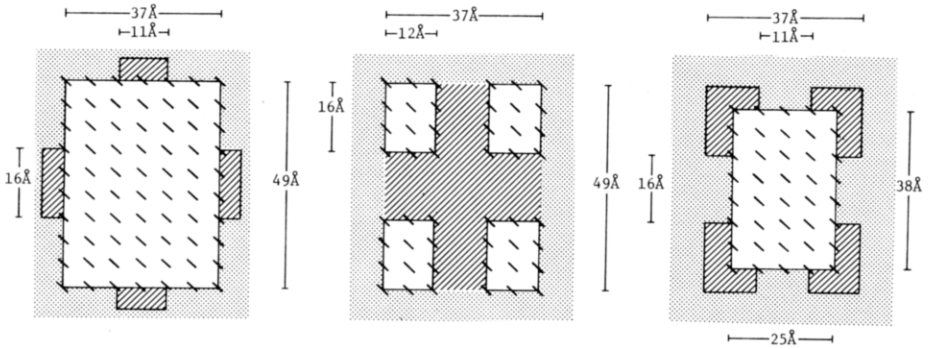

FIG. 22. Cross-sectional models for the 37 × 49Å spiral microfibril (1 mm ≃ 1Å), showing the crystalline cellulose (clear), associated protein (////), and coating material ( ).

negative stain prior to drying, possibly giving a closer approximation to the wet state than the data from x-ray diffraction. Finally, the negatively stained image of the microfibril varies along its length, in that the dark central band is not always visible. While this observation could be explained by a slight twisting of the microfibril, it is generally accepted that the structure of the crystalline core of cellulose microfibrils is not continuous throughout its length [37], with even some evidence for cross-links or anastomoses between adjacent structural units [35]. X-ray line-broadening would yield an average crystallite size, while with negative staining the investigator would tend to select particular areas over others. Thus, the question of the supermolecular structure of scale cellulose is reduced to the same dichotomy that has existed for almost two decades since the original proposals of the solid core [38] and "elementary fibril" models [12]. The persistence of this dichotomy is due, in part, to fundamental differences between electron microscopy and x-ray diffraction as experimental techniques, as well as the apparent diversity of the microfibrillar macromolecules that are called cellulose. However, due to the unique organization of the scale, this study presents an unequivocal demonstration of 40–50Å cellulose microfibrils supported both by negative staining and x-ray diffraction, which cannot be refuted on the basis of disruptive isolation techniques [7] or interference resulting from overlapping images [36].

CONCLUSIONS

In the past, two lines of reasoning have been used to dispute Golgi-mediated cellulose synthesis in *Pleurochrysis:* (1) the scales do not contain cellulose, or (2) synthesis is not completed within the Golgi apparatus. Considering the evidence contained in this present study, both statements have been shown to be false. Thus, there can be no doubt that the synthesis of cellulose microfibrils reaching 14 μm in length occurs within the cisternae of the Golgi apparatus, a conclusion that is at odds with the widely held belief that cellulose synthesis occurs only at or outside of the cell surface [7,37]. Van Der Woude et al. [45] have explained the presence of in vitro β-1, 4-glucan synthetase in Golgi fractions by suggesting that this enzyme may remain inactive until the flow of membrane to the cell surface, i.e. that the Golgi apparatus transports the glucan synthetase to the plasma mem-

brane. Viewed in light of this suggestion, cellulose synthesis in *Pleurochrysis* simply requires that the glucan synthetase become active while still within the Golgi apparatus. The focus of this discussion is not to imply that cellulose is synthesized within the Golgi apparatus in all plants, but rather that such synthesis does occur. Thus, the verification of cellulose biosynthesis by the endomembrane system has forced a reevaluation of the current theory that the plasma membrane is the exclusive site of cellulose biosynthesis in plant cells.

We believe that this study emphasizes the importance of model systems which permit specific conclusions not otherwise attainable. For example, with *Pleurochrysis* it has been possible not only to demonstrate cellulose synthesis within the endomembrane system, but also to determine the rate of cellulose biosynthesis on the basis of morphological evidence, the first such attempt with a eukaryotic system. Brown [2] estimated that one cisterna is produced approximately every two minutes, which means that the five cisternal differentiations necessary to synthesize the spiral microfibrils of a single scale [5] would require approximately ten minutes. Considering that the scale is composed of approximately ten spiral microfibrils with a maximum length of 14 μm, and that the maximum number of glucan chains in cross-section would be 70 for the solid core model, the maximum rate of cellulose production would be 10^8 glucose residues per hour. This rate is in agreement with earlier estimates of the rate of cellulose synthesis in *Acetobacter* [19,32], but is ten times greater than the rate calculated more recently by Colvin [7]. Given the approximations involved in these estimations, it is difficult to evaluate the significance of the difference between the *Acetobacter* rate and that of *Pleurochrysis*. However, the rate of cellulose synthesis in *Pleurochrysis* is at least as great as the rate of cellulose synthesis in the bacterium *Acetobacter*.

The authors wish to acknowledge several colleagues for excellent technical assistance and thoughtful discussion in the following areas: Dr. Jacob Hanker of the Dental Research Center, in the preparation of infrared spectra; Dr. Aristotle Domnas of the Botany Department, in the extraction and compositional analysis; and Drs. Richard Bear and Ronald Chandross of the Laboratory of Reproductive Biology, in the x-ray diffraction studies.

REFERENCES

[1] P. Albersheim, W. D. Bauer, K. Keestra, and K. W. Talmadge, in *Biogenesis of Plant Cell Wall Polysaccharides*, F. Loewus, Ed., Academic Press, New York, 1973, p. 117.
[2] R. M. Brown, Jr., *J. Cell Biol., 41,* 109 (1969).
[3] R. M. Brown, Jr., W. W. Franke, H. Kleinig, H. Falk, and P. Sitte, *J. Cell Biol., 45,* 246 (1970).
[4] R. M. Brown, Jr., W. Herth, W. W. Franke, and D. Romanovicz, in *Biogenesis of Plant Cell Wall Polysaccharides*, F. Loewus, Ed., Academic Press, New York, 1973, p. 207.
[5] R. M. Brown, Jr. and D. K. Romanovicz, *Appl. Polym. Symp., 28* (2), 537 (1976).
[6] D. F. Caufield, *Text. Res. J., 41,* 267 (1971).
[7] J. R. Colvin, *CRC Critical Reviews of Macromolecular Sciences* Vol. 1, 1972, p. 47.
[8] J. R. Colvin and G. G. Leppard, *J. Microsc., 11,* 285 (1971).
[9] D. Danon, L. Goldstein, Y. Marikovsky, and E. Skutelsky, *J. Ultrastruct. Res., 38,* 500 (1972).
[10] R. A. B. Drury and E. A. Wallington, *Carleton's Histological Technique,* 4th ed., Oxford Univ. Press, New York, 1967, p. 217.
[11] M. Dubois, K. A. Gilles, J. K. Hamilton, P. A. Rebers, and F. Smith, *Anal. Chem., 28,* 350 (1956).
[12] A. Frey-Wyssling, *Science, 119,* 80 (1954).
[13] J. C. Green and D. H. Jennings, *J. Expl. Botn., 18,* 359 (1967).
[14] D. W. Gregory and B. J. S. Pirie, *J. Microsc., 99,* 251 (1973).

[15] R. H. Haschemeyer and R. J. Meyers, in *Principles and Techniques of Electron Microscopy,* Vol. 2, M. A. Hayat, Ed., Van Nostrand Reinhold, New York, 1972, p. 101.
[16] P. H. Hermans, *Contributions to the Physics of Cellulose Fibers,* Elsevier, New York, 1946, p. 56.
[17] W. Herth, W. W. Franke, J. Stadler, H. Bittiger, G. Keilich, and R. M. Brown, Jr., *Planta, 105,* 79 (1972).
[18] W. Herth, W. W. Franke, H. Bittiger, A. Kuppel, and G. Keilich, *Cytobiol., 9,* 344 (1974).
[19] S. Hestrin and M. Schramm, *Biochem. J., 58,* 345 (1954).
[20] F. W. Jones, *Proc. Roy. Soc., A1,16,* 16 (1938).
[21] H. P. Klug and L. E. Alexander, *X-Ray Diffraction Procedures,* Wiley, New York, 1954, p. 491.
[22] D. T. A. Lamport, *Ann. Rev. Plant Physiol., 21,* 235 (1970).
[23] D. T. A. Lamport, in *Biogenesis of Plant Cell Wall Polysaccharides,* F. Loewus, Ed., Academic Press, New York, 1973, p. 149.
[24] C. Y. Liang and R. H. Marchessault, *J. Polym. Sci., 37,* 385 (1959).
[25] A. G. Lloyd, K. S. Dodgson, R. G. Price, and F. A. Rose, *Biochim. Biophys. Acta, 46,* 108 (1961).
[26] H. J. Marrinan and J. Mann, *J. Polym. Sci., 21,* 301 (1956).
[27] E. R. McCall, N. M. Morris, V. W. Tripp, and R. T. O'Connor, *Appl. Spectrosc., 25,* 196 (1971).
[28] A. J. Mitchell and G. Scurfield, *Aust. J. Biol. Sci., 23,* 345 (1970).
[29] M. L. Nelson and R. T. O'Connor, *J. Appl. Polym. Sci., 8,* 1325 (1964).
[30] I. Nieduszynski and R. D. Preston, *Nature, 225,* 273 (1970).
[31] R. T. O'Connor, E. F. Dupre, and D. Mitcham, *Text. Res. J., 28,* 382 (1958).
[32] I. Ohad, D. Danon, and S. Hestrin, *J. Cell Biol., 12,* 31 (1962).
[33] R. S. Orr, L. C. Weiss, H. B. Moore, and J. N. Grant, *Text. Res. J., 25,* 592 (1955).
[34] B. Parker and A. G. Diboll, *Phycologia, 6,* 37 (1966).
[35] A. Peterlin and P. Ingram, *Text. Res. J., 40,* 345 (1970).
[36] R. D. Preston, *J. Microsc., 93,* 7 (1971).
[37] R. D. Preston, *The Physical Biology of Plant Cell Walls,* Chapman and Hall, London, 1974.
[38] R. D. Preston and J. Cronshaw, *Nature, 181,* 248 (1958).
[39] H. Rosen, *Arch. Biochem. Biophys., 67,* 10 (1957).
[40] D. Sadava and M. J. Chrispeels, *Science, 165,* 299 (1969).
[41] D. Sadava and M. J. Chrispeels, in *Biogenesis of Plant Cell Wall Polysaccharides,* F. Loewus, Ed., Academic Press, New York, 1973, p. 165.
[42] L. Segal, J. J. Creely, A. E. Martin, Jr., and C. M. Conrad, *Text. Res. J., 29,* 786 (1959).
[43] E. W. Thompson and R. D. Preston, *J. Exp. Bot., 19,* 690 (1968).
[44] M. Tsuboi, *J. Polym. Sci., 25,* 159 (1957).
[45] W. J. Van Der Woude, C. A. Lembi, D. J. Morré, J. I. Kindinger, and L. Ordin, *Plant Physiol., 54,* 333 (1974).
[46] R. G. Zhbankov, *J. Polym. Sci. Part C, 16,* 4629 (1969).